Interlayer Structure and Dynamics of ClO_4^- Layered Double Hydroxides

Xiaoqiang Hou* and R. James Kirkpatrick

Department of Geology, University of Illinois at Urbana−Champaign, Urbana, Illinois, 61801

Received August 8, 2001. Revised Manuscript Received January 7, 2002

This paper presents a ^{35}Cl NMR and XRD study of the structure and dynamical behavior of ClO_4^- intercalated into the interlayers of Mg,Al and Li,Al layered double hydroxides (LDHs). The variable temperature and variable relative humidity (R.H.) ^{35}Cl NMR data show that for these phases ClO_4^- is rigidly held at low R.H.'s and temperatures, but that at high R.H.s and in pastes at room temperature it undergoes isotropic reorientation at frequencies $>10^3$ Hz. Surface and interlayer ClO_4^- cannot be distinguished. The dynamical behavior is similar for both phases, even though the Li,Al phase swells to a two-water-layer structure but the Mg,Al phase does not. The ^{35}Cl static NMR peak shape is dominated by uniaxial chemical shift anisotropy (CSA) due to the layer structure. These results contrast with previously published ^{77}Se NMR data for interlayer SeO_4^{2-} in comparable Mg,Al and Li,Al LDHs, which show that SeO_4^{2-} does not undergo isotropic reorientation at any R.H. SeO_4^{2-} and ClO_4^- have similar tetrahedral structures and ionic radii, and we attribute the difference in their dynamical behavior to the difference in ionic charge and the corresponding differences in electrostatic and hydrogen bonding between the anions and the hydroxide layer and interlayer water molecules.

Introduction

Understanding the molecular-scale structure and dynamics of interlayer and surface species in layered double hydroxides (LDHs) is essential to prediction and analysis of their exchange behavior[1−3] and to many of their applications[4] and provides important perspective on the fundamental structural and dynamic behavior of surface and interlayer species in layer-structure materials.[1−9] Layered double hydroxides have permanent, positive charges and, thus, significant anion-exchange capacities.[4,10] They have wide-ranging potential applications as catalysts, filtration, and exchange materials and in drug and gene delivery systems.[4,11] They are also increasingly being identified in natural environments and hazardous waste sites.[12,13] The crystal structures of LDHs consist of positively charged hydroxide sheets separated by interlayers containing exchangeable anions and water molecules.[4] Their structures can be thought to be derived from either a trioctahedral brucite-like structure or a dioctahedral gibbsite-like structure. In the former case, LDHs develop their net positive charge by isomorphous substitution of, for example, Al^{3+} for Mg^{2+} on octahedral sites.[14] In the latter case, for which only the Li,Al compounds have been reported, Li^+ occupies the octahedral vacancies of the gibbsite sheet.[15,16]

We present here a ^{35}Cl NMR and XRD study of the behavior of the perchlorate ion, ClO_4^-, in Mg,Al and Li,-Al LDHs. Relative to other common oxyanions, perchlorate has a low charge and large ionic radius and is thus expected to undergo reorientational dynamics more easily than other species that have been studied.[2,3] Here, we focus especially on the differences between the ClO_4^- and SeO_4^{2-},[3,17] which is an effective model for SO_4^{-2} in LDHs. SeO_4^{2-} and ClO_4^- have similar ionic radii[18] (0.243 vs 0.240 nm), but different charges. Both species have nominal T_d symmetry, but distortion from this

* To whom correspondence should be addressed. Phone: (217) 244-2355. Fax: (217) 244-4996. E-mail: xhou@uiuc.edu.

(1) Kirkpatrick, R. J.; Yu, P.; Hou, X.-Q.; Kim, Y. *Am Mineral.* **1999**, *84* (7−8), 1186.
(2) Hou, X.-Q.; Kirkpatrick, R. J.; Yu, P.; Moore, D.; Kim, Y. *Am. Mineral.* **2000**, *85*, 173.
(3) Hou, X.-Q.; Kirkpatrick, R. J. *Chem. Mater.* **2000**, *12* (7), 1890−1897.
(4) Cavani, F.; Trifiro, F.; Vaccari, A. *Catal. Today* **1991**, *11*, 173.
(5) Dupuis, J.; Battut, J. P.; Fawal, Z.; Hajjimohamad, H.; De Roy, A.; Besse, J. P. *Solid State Ionics* **1990**, *42* (3−4), 251−255.
(6) Menetrier, M.; Han, K. S.; Guerlou-Demourgues, L.; Delmas, C. *Inorg. Chem.* **1997**, *36* (11), 2441−2445.
(7) van der Pol, A.; Mojet, B. L.; van de Ven, E.; de Boer, E. *J. Phys. Chem.* **1994**, *98* (15), 4050−4054.
(8) Maxwell, R. S.; Kukkadapu, R. K.; Amonette, J. E.; Cho, H. *J. Phys. Chem. B* **1999**, *103* (25), 5197−5203.
(9) Marcelin, G.; Stockhausen, N. J.; Post, J. F. M.; Schutz, A. *J. Phys. Chem.* **1989**, *93* (11), 4646−4650.
(10) Bish, D. L. *Bull. Mineral.* **1980**, *103*, 170−175.
(11) Choy, J.-H.; Kwak, S.-Y.; Park, J.-S.; Jeong, Y.-J.; Portier, J. *J. Am. Chem. Soc.* **1999**, *121* (6), 1399−1400.
(12) Gade, B.; Riedmiller, J.; Westerrmann, H.; Heindl, A.; Pollmann, H. *Neues Jahrb. Mineral., Abh.* **1999**, *174* (3), 249−275.
(13) Genin, J.-M. R.; Refait, P.; Bourrie, G.; Abdelmoula, M.; Trolard, F. *Appl. Geochem.* **2001**, *16* (5), 559−570.
(14) Bellotto, M.; Rebours, B.; Clause, O.; Lynch, J.; Bazin, D.; Elkaiem, E. *J. Phys. Chem.* **1996**, *100*, 8527.
(15) Besserguenev, A. V.; Fogg, A. M.; Francis, R. J.; Price, S. J.; O'Hare, D.; Isupov, V. P.; Tolochko, B. P. *Chem. Mater.* **1997**, *9*, 241−247.
(16) Isupov, V. P.; Gabuda, S. P.; Kozlova, S. G.; Chupakhina, L. C. *J. Struct. Chem.* **1998**, *39* (3), 362−366.
(17) Hou, X.-Q. Structure and Dynamics of Layered Double Hydroxides. Ph.D. thesis, University of Illinois at Urbana-Champaign, 2001.
(18) Moyer, B. A.; Bonnesen, P. V. In *Supramolecular Chemistry of Anions*; Bianchi, A., Bowman-James, K., Garcia-Espana, E., Eds.; John Wiley & Sons Inc.: New York, 1997.

10.1021/cm0107474 CCC: $22.00
Published on Web 02/28/2002

high symmetry in the LDH interlayers due to electrostatic and H-bonding effects causes development of chemical shift anisotropy (CSA) at the central atom, ^{35}Cl or ^{77}Se, providing an effective element-specific probe of the structure and dynamics.[3,17] This effect is comparable to the peak splitting observed in vibrational (IR and Raman) spectra of similar LDHs.[19] In addition, NMR spectroscopy uniquely probes the relatively low-frequency dynamics of the anions.[1−3]

Experimental Section

Sample Preparation. The ClO_4 Mg,Al sample used in this study was made by exchanging ClO_4^- into NO_3 Mg,Al LDH that had been previously prepared using a coprecipitation method.[2,19] Nine grams of dried NO_3 Mg,Al sample was added to 400 mL of 0.5 M $KClO_4$ solution to allow exchange at 20 °C under vigorous stirring for 19 h. The mixture was washed and placed into boiled DI water and then hydrothermally treated under autogenous pressure in a Parr vessel for 72 h at 190 °C to increase the particle size. The resulting product was dried in a vacuum oven at room temperature for 3 weeks. Attempts to exchange ClO_4^- for CO_3^{2-} and Cl^- in Mg,Al LDH failed even at acidic conditions.[10,20−22] ClO_4 Li,Al LDHs were prepared by both direct intercalation[23] and exchange reaction. For direct intercalation, 18 g of gibbsite and 100 g of $LiClO_4 \cdot 3H_2O$ dissolved in 50 mL of DI water were mixed and reacted at 90 °C for 7 days in a tightly sealed polyethylene bottle under strong stirring.[23] The suspension was then allowed to continue to react without stirring at 90 °C for another 30 h. The mixture was then washed 3 cycles with hot DI, N_2-fluxed water to remove excess $LiClO_4$. For exchange synthesis, NO_3^- Li,Al LDH was added to 2 M $KClO_4$ solution and allowed to react under strong stirring for 20 h at 50 °C.

Sample Examination. Samples were examined by elemental analysis, XRD, and ^{35}Cl static and MAS NMR. For elemental analysis, Li, Al, and Mg were determined using inductively coupled plasma emission spectroscopy (ICP), C, H, and N were determined with a CHN analyzer, and Cl^- was determined by titration. Powder XRD patterns were recorded for newly made paste, samples air-dried at room temperature or 100 °C, and pastes made by rehydrating samples previously air-dried at 70 °C. A Rigaku diffractometer, Cu Kα radiation, a scanning rate of 3°−1° 2θ/min, and a step size of 0.02°−0.05° 2θ were used.

^{35}Cl NMR spectra were collected under both static and MAS conditions using a Varian INOVA 750 spectrometer (H_0 = 17.62 T) and a home-built 500-MHz spectrometer (H_0 = 11.74 T) equipped with a Tecmag Aries data system. Doty Scientific fast MAS probes were used in all cases. Static spectra were collected using a 90°−τ −180° echo pulse sequence. MAS spectra were collected using a single-pulse sequence with 16-step phase cycling. Samples included newly made pastes, aliquots equilibrated at controlled R.H.s., aliquots heated at 60 and 150 °C in air, and pastes made from DI water and LDH previously dried at room temperature in a vacuum oven. For spectra collected at room temperature and controlled R.H., the samples were placed in open containers in a sealed desiccator or glovebag, equilibrated for at least 4 days over saturated salt buffers,[24] and quickly loaded into glass tubes or MAS rotors and sealed with epoxy or rotor caps just prior to data collection. The 0% R.H. sample was obtained by equilibrating it over P_2O_5 for 3 weeks. Heated samples were also quickly loaded just prior to data collection to avoid moisture absorption. In situ variable temperature spectra were collected from +100 to −98 °C using a liquid-nitrogen cooling system and a resistance heating system.[1−3] NaCl (1 M) in aqueous solution was used as an external chemical shift standard for ^{35}Cl, and its chemical shift was set at 0 ppm. Typically, a recycle time of 1 s was used.

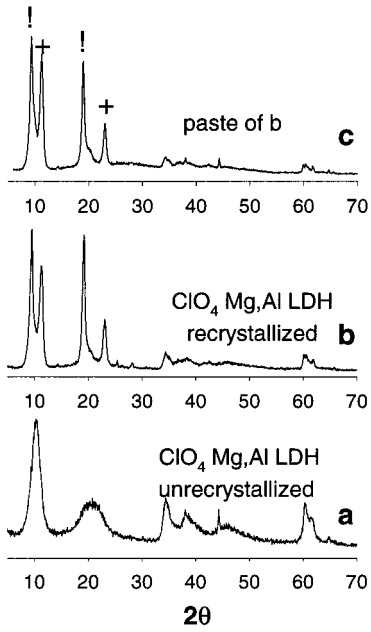

Figure 1. Powder XRD patterns of ClO_4^- Mg,Al LDHs prepared by exchange of ClO_4^- for NO_3^- at room temperature for 17 h. See text for details. (a) Unrecrystallized, dried. (b) Hydrothermally recrystallized at 190 °C for 3 days, dried. (c) Rehydrated paste of (b), showing that there is no significant swelling for the Mg,Al phases. ! = ClO_4^- Mg,Al LDH; + = CO_3^{2-} Mg,Al LDH.

Results and Spectral Interpretation

Synthesis, Composition, and XRD Powder Patterns. Pure ClO_4^- LDHs are difficult to prepare due to the low affinity of ClO_4^- for both the Mg,Al and Li,Al phases. For the Mg,Al phase, exchange and recrystallization produced the best sample, which had the composition $Mg_{0.73}Al_{0.27}(OH)_2(ClO_4)_{0.15}(CO_3)_{0.06} \cdot 0.40H_2O$ on limit, and this sample was used for all subsequent experiments. The ^{27}Al MAS NMR spectrum of this sample shows only LDH and is identical to those previously published.[25] The XRD confirms this result and the pattern for the recrystallized sample confirms our previous observation that different anions tend to form separate LDH phases rather than mix in individual interlayers to form solid solutions (Figure 1).[3] The carbonate in this phase is due to impurity in the starting NO_3^- LDH and/or contamination during exchange and subsequent hydrothermal treatment. For the Li,Al phase, direct reaction of gibbsite with $LiClO_4$ solution for 7 days produces very pure LDH (Figure 2a−c) with a structural formula of $Li_{0.78}Al_{2.22}(OH)_6.(ClO_4)_{0.82} \cdot 1.54H_2O$. The ^{27}Al and ^{6}Li MAS NMR spectra of this sample show a signal from only LDH and are essentially identical to that of Cl Li,Al LDH.[26] The analyzed atomic Al/Li ratio is larger than 2, as we have previously observed for Cl Li,Al LDH due to incomplete reaction of the gibbsite.[26] The slow incorporation of $LiClO_4$ into

(19) Miyata, S. *Clays Clay Miner.* **1975**, *23*, 369.
(20) Drezdzon, M. A. *Inorg. Chem.* **1988**, *27* (25), 4628−4632.
(21) Kukkadapu, R. K.; Witkowski, M. S.; Amonette, J. E. *Chem. Mater.* **1997**, *9*, 417−419.
(22) Brindley, G. W.; Kikkawa, S. *Am. Mineral.* **1979**, *64*, 836−843.
(23) Fogg, A. M.; O'Hare, D. *Chem. Mater.* **1999**, *11*, 1771−1775.
(24) Lide, D. R. *CRC Handbook of Chemistry and Physics*, 79th ed; CRC Press: Boca Raton, FL, 1998.
(25) MacKenzie, K. J. D.; Meinhild, R. H.; Sherriff, B. L.; Xu, Z. *J. Mater. Chem.* **1993**, *3* (12), 1263−1269.
(26) Hou, X.; Kirkpatrick, R. J. *Inorg. Chem.* **2001**, *40* (25), 6397−6404.

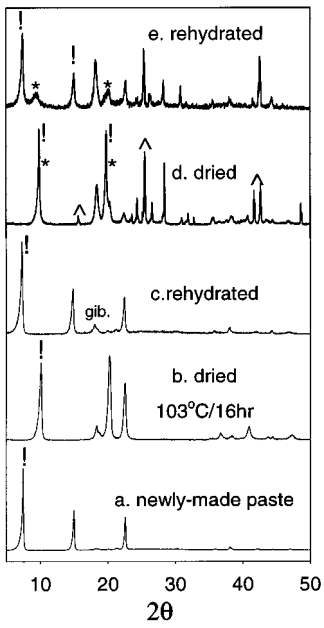

Figure 2. (a−c) Powder XRD patterns of ClO_4^- Li,Al LDHs prepared by direct reaction of gibbsite with $LiClO_4$ at 90 °C for 7 days: (a) newly made paste; (b) dried at 100 °C/16 h; (c) rehydrated paste. (d, e) ClO_4^- Li,Al LDHs prepared by exchange ClO_4^- for NO_3^- at 50 °C for 20 h: (d) dried; (e) rehydrated paste. ! = ClO_4^- Li,Al LDH; * = residual NO_3^- Li,-Al LDH; ∧ = $KClO_4$.

gibbsite contrasts with the behavior of other anionic species, which react readily,[23] and is one example of the effects of the low charge and large ionic radius of ClO_4^-. The exchange of ClO_4^- for NO_3^- in Li,Al LDH did not yield pure ClO_4^- Li,Al LDH (Figure 2d,e) and the obtained sample was not used for ^{35}Cl NMR data collection.

Expansion and contraction of the basal spacings with wetting and drying and variation in R.H. have been observed for several LDHs[3,17,27] and is important for understanding the structural and dynamical behavior of the interlayer anions. Here, ClO_4 Li,Al LDH swells significantly, but ClO_4 Mg,Al LDH does not. The basal spacing of the Li,Al phase is 11.81 Å for the as-made paste, decreases to 8.73 Å for the dried sample, and re-expands to 12.1 Å for a rehydrated sample (Figure 2a−c). The expansion corresponds to a structural transformation from a partially occupied one-water-layer structure to a two-water-layer structure,[27] as also observed for SeO_4 Mg,Al LDH[3] and SeO_4 Li,Al LDH.[17] The 12.1-Å *d* spacing for the fully hydrated perchlorate phase, however, is ≈1.0 Å greater than that of both SeO_4 Li,Al and SeO_4 Mg,Al LDHs. ClO_4 Mg,Al LDH does not swell significantly, and the *d* spacing difference between the room humidity and paste samples is only 0.1 Å (9.30 vs 9.40 Å, Figure 1b,c).

Comparison of water sorption and XRD data under controlled R.H. conditions[27] shows that in both the ClO_4 Mg,Al and ClO_4 Li,Al phases water molecules occupy interstices between ClO_4^- anions at low R.H. (0−30%) and that this water does not cause significant basal spacing expansion in this R.H. range. The O atoms of the anions are H-bonded to the hydroxyl layers on either side of the interlayer under these conditions. At higher R.H. (≈60%) the ClO_4 Li,Al phase accepts a second water layer, resulting in the observed swelling. Detailed structural and dynamical understanding of the origin of these differences will require molecular dynamics modeling (MD) of these phases, but recent MD simulations of the Cl Li,Al, Mg,Al, and Ca,Al LDHs suggest that competition of the anions and water for sites next to the OH groups and the consequent effects on the interlayer H-bond network are likely to play prominent roles.[28−30] In the Mg,Al phases the water molecules are strongly attracted to the hydroxide layer, forming two sublayers with the anions in the center of the interlayer.[29] Many of the O atoms of the water molecules coordinate Mg in the hydroxide layer, forming a stable configuration. In contrast, the water molecules in the Li,Al phases cannot coordinate the cations and in the one-water-layer structure for the Cl phase remain in the center of the interlayer with the anions.[15,30] For the large, low-charge ClO_4^- anion, this structural difference is likely to cause substantial differences in the interlayer H-bond network and its ability to accept a second layer of waters.

^{35}Cl NMR. *Room Temperature ^{35}Cl NMR of $LiAl_2(OH)_6ClO_4 \cdot nH_2O$ under Variable R.H.* The room temperature (RT) static ^{35}Cl NMR spectra of the ClO_4 Li,Al LDH (Figure 3, left column) contain signal from only one resonance. At low R.H. the line shapes are dominated by uniaxial chemical shift anisotropy (CSA; Figure 3a−e), but at R.H.s above 75% the peaks are narrower and symmetric (Figure 3f−h). The CSA patterns for the samples equilibrated at 0% R.H. and at 150 °C (Figures 3a, b) can be well-fitted with a uniaxial CSA pattern with principal components of $\delta_{||} = 1019$ ppm, $\delta_{\perp} = 987$ ppm, and $\delta_i = 997.7$ ppm. The corresponding MAS spectra (Figures 3i, j) have peak maxima at 997.2 ppm, in good agreement with the simulated δ_i. The MAS spectrum for the 150 °C sample, however, is not symmetric and probably includes some unaveraged second-order quadrupolar broadening. It can be well-simulated with a quadrupole coupling constant (QCC) of 0.7 MHz, an asymmetry parameter (η) of 0.1, and an isotropic line broadening of 160 Hz. At R.H. = 11% the static spectrum is narrower and can be well-simulated with $\delta_{||} = 1007$ ppm, $\delta_{\perp} = 994$ ppm, and $\delta_i = 998.3$ ppm. The corresponding MAS spectrum contains a single symmetrical peak with a maximum at 998.7 ppm, again in excellent agreement with the simulated δ_i. The static spectra for the 33% R.H. and 51% R.H. samples are similar to that at 11% R.H. but slightly narrower (e.g., $\delta_{||} = 1004$ ppm, $\delta_{\perp} = 995$ ppm, and $\delta_i = 998$ ppm at R.H. = 51%). The corresponding MAS spectra have peak maxima at 998.8 and 997.8 ppm, respectively, in excellent agreement with the simulations (Figure 3k,l,m). Both the MAS and static spectra for the 75% R.H., 84% R.H., and paste samples are narrow symmetric peaks with maxima at ≈999.3 ppm. The static spectrum of the paste is narrower (fwhh = 132 Hz) than the others

(27) Hou, X.; Bish, D. L.; Wang, S.-l.; Johnston, C.; Kirkpatrick, R. J. *Am. Mineral.*, submitted.

(28) Kalinichev, A. G.; Kirkpatrick, R. J.; Cygan, R. T. *Am. Mineral.* **2000**, *85*, 1046−1052.

(29) Wang, J.-W.; Kalinichev, A. G.; Kirkpatrick, R. J.; Hou, X.-Q. *Chem. Mater.* **2001**, *13* (1), 145−150.

(30) Hou, X.-Q.; Kalinichev, A. G.; Kirkpatrick, R. J. *Chem. Mater.*, submitted.

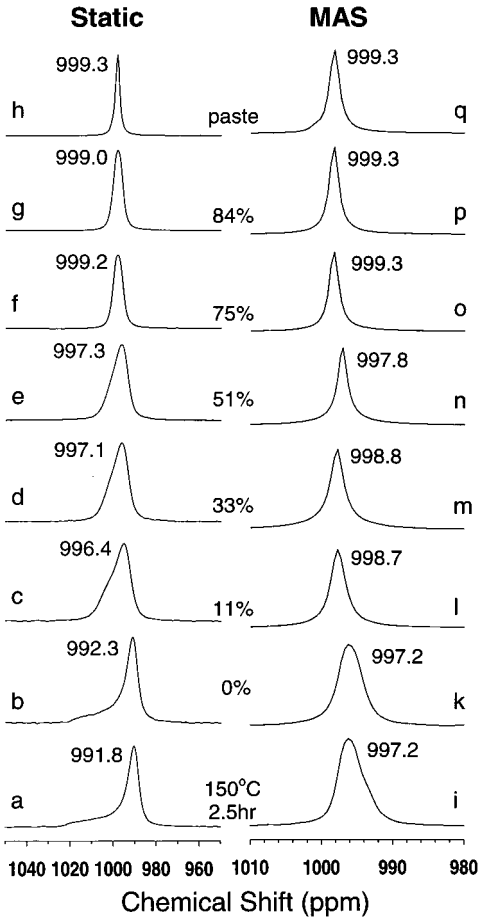

Figure 3. Static and MAS ^{35}Cl NMR spectra of $LiAl_2(OH)_6ClO_4 \cdot nH_2O$ treated at the relative humidities (R.H.'s) indicated. The % values are R.H., and other values given are observed peak maxima. Data collected at $H_0 = 17.6$ T.

(fwhh's = 354 and 342 Hz, respectively) but has the same peak maximum.

The observed uniaxial CSA patterns for perchlorate at low R.H. indicate distortion from its ideal T_d symmetry due to external bonding effects. Isolated $^{35}ClO_4^-$ would yield only a symmetrical peak due to this high symmetry. Previous studies of perchlorate LDH using IR[19] spectroscopy have suggested that interlayer ClO_4^- is distorted from tetrahedral symmetry, but the results are not as convincing and unambiguous as in the NMR because of band overlap and low resolution. Miyata[19] suggested that perchlorate is cross-linked to the hydroxyl layer through Cl−O−M (M = metals) bonds. However, the similarity of the isotropic chemical shifts of interlayer $^{35}ClO_4^-$ and $^{35}ClO_4^-$ in solution (997.4 ppm; Figure 4l), the reversibility of the basal spacing expansion, and the reorientational dynamics discussed below clearly indicate that this cross-linking does not occur. The distortion must be due to the combined effects of hydrogen bonding of the oxygens of the perchlorate to the OH groups of the octahedral layers and interlayer water molecules and to Coulombic interaction with the hydroxide layers. A reduction in $|\delta_\perp - \delta_{||}|$ implies either a smaller anisotropic bonding effect or peak narrowing due to reorientation of the CSA tensor at frequencies of the order of the static peak width ($\approx 10^3$ Hz). On the basis of the XRD results described above, TG/DSC data that show loss of water beginning near room temperature at heating rates of 10 °C/min and IR data for

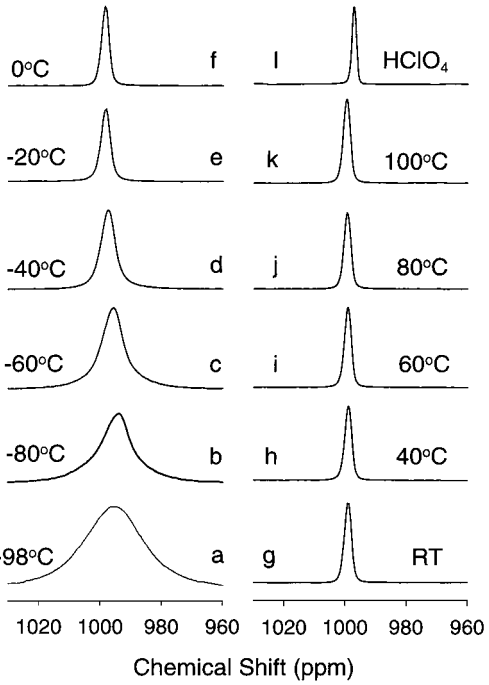

Figure 4. Variable temperature, static ^{35}Cl NMR spectra of paste $Mg_3Al(OH)_6ClO_4 \cdot nH_2O$ collected at the indicated in situ temperatures at $H_0 = 11.7$ T. The upper right spectrum is for $HClO_4$ acid (70% w/w). See text for details.

samples equilibrated at ≈0% R.H. that show the absence of water bending bands (our unpublished data), the 150 °C and 0% R.H. samples are fully or nearly fully dehydrated. Thus, their ClO_4^- forms hydrogen bonds with only the hydroxyl groups from the hydroxide layers on either side and is probably rigidly held in the interlayer. At R.H.'s from 11% to 51%, this LDH has a one-water-layer structure, with the water molecules in the interstices between the ClO_4^-.[27] Once water is present in the interlayer, the ClO_4^- forms hydrogen bonds with the water molecules,[28] resulting in a CSA pattern with a smaller $\Delta\delta$. The reduction in $|\delta_\perp - \delta_{||}|$ under these conditions may be both structural and dynamical in origin. H-bonding to the interlayer waters may change the components of the shielding tensor. Reorientation of the shielding tensor due to, for example, librational hopping of the water molecules among equivalent H-bonding positions[28,30] and isotropic or anisotropic rotation of the ion could also lead to similar spectra. It is currently not possible to distinguish between these possibilities. At R.H. of 75% and higher, the narrow symmetrical static peaks and the similar widths of the static and MAS peaks show that the ClO_4^- must be in a more or less solution-like environment and that the narrowing is effected substantially by isotropic reorientation. Molecular dynamics modeling of the two-water layer structure present at these high R.H.'s will be needed to fully define the structural environments and rotational dynamics, including the origin of the ≈1 Å greater basal spacing for fully hydrated ClO_4 Li,Al phase relative to SeO_4 Li,Al and Mg,Al phases.[3,17,27]

Assuming that the line narrowing with increasing R.H. is purely of dynamical origin, the perchlorate reorientation frequencies can be determined using the method we have previously applied to other anions in LDHs.[2,3] The experimental line width, β, obeys the

following equation:

$$(\beta^2 - \beta_h^2)/(\beta_l^2 - \beta_h^2) = 2/\pi \arctan(\beta/\nu_c) \qquad (1)$$

where β_h and β_l are the smaller and larger limits for β in a systematically controlled variable regime such as temperature or R.H. and ν_c is the reorientational frequency (1/correlation time) to be determined. We take β_h to be 70 Hz (fwhh of the $KClO_4$ solution), and β_l to be the static peak width ($|\delta_\perp - \delta_{||}|$) for the sample dried at 150 °C. Using this method, the reorientation frequencies, ν_c, are 5.4 kHz for the 51% R.H. sample and 37.1 kHz for the paste. The value for the paste is more than an order of magnitude larger than that for SeO_4^{2-} (≈2.0 kHz) under similar conditions.[3] This difference illustrates well the effects of the smaller charge (electrostatic interaction) of the perchlorate. Fully hydrated SeO_4^{2-} Mg,Al LDH[3] and SeO_4^{2-} Li,Al LDH[17] both show well-defined static $^{77}SeO_4^{2-}$ CSA patterns at room temperature, even though both swell to a two-water-layer structure.[27] A decreasing CSA with increasing temperature[3] confirms the effects of rotational dynamics on the $^{77}SeO_4^{2-}$ spectra. Because selenate and perchlorate have similar ionic radii and tetrahedral structures, the difference in their dynamical behavior in LDHs and their effect on the basal spacings must be due to their different charges and thus to differences in their Coulombic attraction to the hydroxide layers and H-bonding behavior. Tetrahedral anions can take on uniaxial symmetry in LDHs with either of two orientations,[10,22,31] $C_2||c$ (two of the four oxygens up and two down) or $C_3||c$ (three oxygens up and one down or vice versa). Changing interlayer water content due to changing R.H. may induce a change in orientation, but we cannot determine this with present data, and molecular dynamics modeling will be useful in this regard.[28, 29]

^{35}Cl NMR of $Mg_3Al(OH)_6ClO_4{\cdot}nH_2O$. The R.H. dependence of the ^{35}Cl NMR spectra of $Mg_3Al(OH)_6ClO_4{\cdot}nH_2O$ is very similar to that for $LiAl_2(OH)_6ClO_4{\cdot}nH_2O$, even though the ClO_4 Mg,Al compound does not expand to a two-water layer structure. For the sample dehydrated at 150 °C (Figure 5a) and at R.H. = 0% (Figure 5b), the line shapes are dominated by CSA. The spectrum of the 150 °C heated sample is well-simulated with $\delta_{||} = 1012$ ppm, $\delta_\perp = 997$ ppm, and $\delta_i = 1002$ ppm, in good agreement with the observed MAS peak maximum at 1001.2 ppm (data not shown). The spectrum of the room humidity sample shows a very small CSA (Figure 5c) and that of the paste sample shows only a narrow symmetric peak with a fwhh of 113 Hz (Figure 5d). As for the ClO_4 Li,Al sample discussed above, variation in the hydration state may affect both the static CSA values and the rotational dynamics.

The variable temperature static ^{35}Cl spectra for ClO_4 Mg,Al LDH paste demonstrate the importance of dynamical effects in these materials. The resonances are featureless and symmetrical, and they narrow progressively with increasing temperature (Figure 4). The fwhh varies from 1001 Hz at −98 °C to 242 Hz at −0 °C to 110 Hz at 40 °C and remains essentially constant up to 100 °C. (The data processing line broadening was 25 Hz.) This is the effect expected for a thermally activated process causing an increasing frequency of reorientational motion with increasing temperature, as previously observed for a number of surface and interlayer anions in LDHs.[1−3] This motion must average line-broadening effects including the dipolar, quadrupolar, and CSA interactions and must involve relative reorientational motion of the ClO_4^- with respect to the main layers and interlayer water molecules. The reorientation frequency can be estimated from the temperature dependence of the NMR peak width using eq 1. Here, the reorientational frequency ν_c (1/correlation time) varies with temperature as[2,3]

$$\nu_c = \nu_0 \exp(-E_a/kT) \qquad (2)$$

Again, we take β_h to be 70 Hz (fwhh of solution), but β_l to be the static peak width at −98 °C, 1001 Hz, to be conservative. The peak could be even broader at lower temperature, which would increase the calculated frequencies, more at lower temperatures, and decrease the activation energy. The calculated ν_c values from eq 1 are in the range 10^2−10^5 Hz and are plotted as a function of temperature in Figure 6. The fit of ν_c to eq

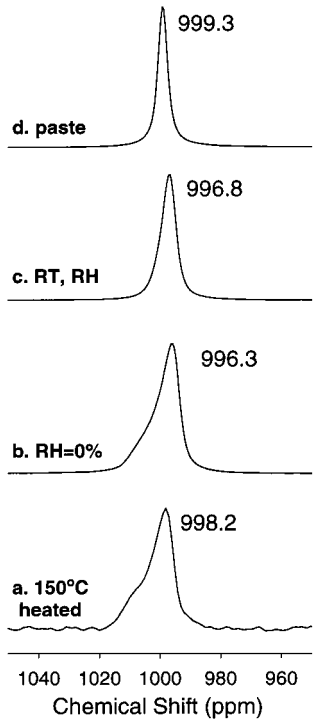

Figure 5. Static ^{35}Cl NMR spectra of $Mg_3Al(OH)_6ClO_4{\cdot}nH_2O$ treated under the conditions indicated. Data collected at H_0 = 11.7 T.

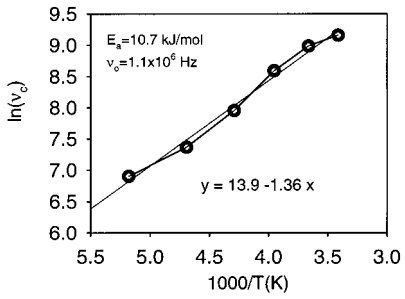

Figure 6. Ahrrenius plot of the ClO_4^- reorientaion frequency of a paste sample of $Mg_3Al(OH)_6ClO_4{\cdot}nH_2O$.

(31) Brindley, G. W.; Kikkawa, S. *Clays Clay Miner.* **1980**, *28* (2), 87−91.

2 yields an apparent activation energy E_a of 10.7 kJ/mol and a ν_0 of 1.1×10^6 Hz. This activation energy is in the range expected for processes controlled by hydrogen bonding and is only slightly smaller than that of SeO_4^{2-} in paste Mg,Al LDH, 11.8 kJ/mol;[3] ν_0 is almost an order of magnitude larger than that of SeO_4^{2-} in paste Mg,Al LDH, 2.3×10^5 Hz, again reflecting smaller Coulombic interaction due to the −1 charge of perchlorate. As indicated above, if a larger β_l was used, the fitted ν_0 would be even larger and E_a would be even smaller. Thus, the argument that the lower charge of ClO_4^- relative to SeO_4^{-2} has a significant effect on the dynamics is not comprised, even if the ^{35}Cl NMR peak width at −98 °C may not be the maximum static peak width.

Acknowledgment. This research is supported by the NSF Grant EAR 95-26317 and DOE Grant DEFG02-00ER15028, R.J.K., principal investigator. We would like to thank Dr. David L. Bish for help with collecting XRD data under controlled relative humidity (R.H.) and Dr. Shan-li Wang for water sorption measurements. Two reviewers' comments and suggestions have improved the manuscript substantially.

CM0107474